Int J Clin Exp Med 2017;10(2):2084-2090
www.ijcem.com /ISSN:1940-5901/IJCEM0035427

Original Article

Luteolin inhibit the cell growth by influencing aminopeptidase N in HepG2

Xingwei Wu[1*], Gang Li[2*], Yong Yang[2], Huan Liu[2], Enwu Long[2]

[1]Department of Clinical Pharmacy, West China School of Pharmacy Sichuan University, Chengdu 610041, China; [2]Department of Pharmacy, Sichuan Academy of Medical Sciences & Sichuan Provincial People's Hospital, Chengdu 610072, China. [*]Equal contributors and co-first authors.

Received July 10, 2016; Accepted October 30, 2016; Epub February 15, 2017; Published February 28, 2017

Abstract: The activity, type and kinetic constant of inhibition on Aminopeptidase N (APN) by luteolin were investigated using the enzyme inhibitory kinetics, the test on hepatoma cell growth inhibition was performed, the interaction between luteolin and APN was investigated by fluorescence quenching and molecular docking, and finally, the effect of luteolin on the structure of APN was discussed. Results showed that luteolin was a reversible competitive inhibitor of APN, with its half maximal inhibitory concentration (IC_{50}) and inhibition constant (K_i) obtained at 70.85 μM and 21.23 μM, respectively. Analysis on the time course of inactivation kinetics revealed that luteolin could react with APN rapidly to reduce the activity of the enzyme. Analysis on fluorescence spectrum indicated that the fluorescence of APN was quenched effectively by luteolin, with hydrophobic interaction force as the main driving force for the interaction between. Analysis of CD spectra revealed that the binding of luteolin to APN could induce conformational unfolding, causing the content of α-helix to increase gradually, hindering formation of the active center and in turn, leading to reduction in the APN activity. Results of molecular simulation showed that luteolin bound in priority to the APN active center of Zn ions, and formed hydrogen bonds with the catalytic groups His383 and Glu384, which indicated that luteolin was a competitive APN inhibitor by reducing the rate of substrate binding to the active center, resulting ultimately in the reduced activity of APN.

Keywords: Luteolin, tumor cells, APN, inhibitory effect, fluorescence spectrum, hepatoma, molecular simulation

Introduction

Growth, invasion and metastasis of tumor is a complex multi-step process, including division and proliferation of tumor cells, degradation of the extracellular matrix, and tumor cells entering into the vascular system through the basement membrane, spreading along with the circulatory system, localized and growing in secondary tissues and organs, and continuous spread of the metastatic carcinoma etc. [1]; Aminopeptidase N (APN) plays an essential part in physiological regulation and signal transmission between tissues and cells in the body, with its function and effects varying depending on its location, and especially, APN plays a role in all of the links in evolution of malignant tumors, e.g. participating in degradation of the extracellular matrix, cardiovascular generation [2-5], degradation of thymosins and interleukins, all of which leads to a reduced immunity of the body and facilitates the growth of tumor, indicating that an APN inhibitor may effectively prevent malignant tumors from transferring and spreading.

Luteolin (**Figure 1**) is a flavanoid and generally present in celery, beef-steak plant leaf, green pepper and camomile tea in the form of glycosylation and also present in perilla seed and parsley in the form of aglycone [6]. Luteolin has the pharmacological activities such as antimutagenic, anti-tumor, anti-infective and antiallergic activities, and is regarded as a free radical scavenger of hydroxide radicals and an inhibitor of protein kinase C. Recent studies revealed that luteolin also had the effects of inhibiting malignant tumor cells and inhibiting the activation of human mast cells [7, 8]. In order to investigate whether the anti-tumor effect of luteolin is related to its inhibitory effect on APN, this article studied the mechanism of

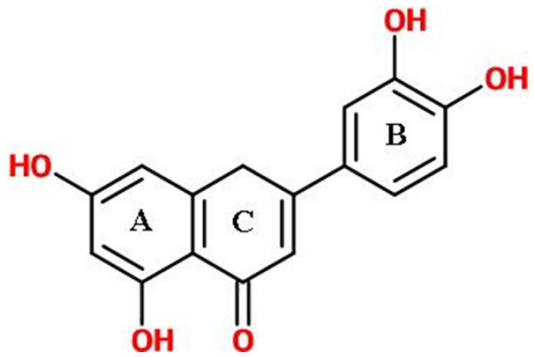

Figure 1. Molecular structure of luteolin.

inhibition of APN by luteolin, analyzed the type of inhibitory effect of luteolin on APN and the inhibition kinetic constants, explored the mechanism of interaction between luteolin and APN and further studied the influence on APN conformation, providing basic data for the development and application of luteolin in the field of functional medicine.

Material and methods

Inhibitory effect of luteolin on APN

The APN catalytic substrate (L-leucine phthalocyanine-p-nitroaniline) generated p-nitroaniline, with ultraviolet absorption at 405 nm, and the concentration of p-nitroaniline was positively related with the size of enzymatic activity; changes in the absorption value at 405 nm were detected to determine the activity of APN, which could indirectly reflect the degree of inhibition on the enzymatic activity [9].

Luteolin (analytically pure, Aladdin reagent) and porcine APN (Sigma Corporation) were incubated at 37°C in the pH 6.8 phosphate (50 mmol/L) buffer system for 3 hours. Afterwards, L-leucine phthalocyanine-p-nitroaniline (analytically pure, Sigma Corporation) was added, the kinetics/time software of UV-2450 type UV-visible spectrophotometer (Japan Shimadzu) was used to detect the changes of absorbance values at 405 nm, and the inhibitory activity of luteolin on APN was calculated with the following formula: relative activity (%) = (R/R_0) × 100%, where, R_0 is the slope rate of changes in absorbance in the absence of inhibitor and R is the slope rate of changes in absorbance in the system containing luteolin at different concentrations. Bestatin (analytically pure, Sigma Corporation) was used as the positive control.

Kinetic study on inhibition of APN by luteolin

In the same buffer system at 37°C, the concentration of APN was fixed, the enzymatic reaction speed was determined at different substrate concentrations, a Lineweaver-Burk plot was drawn, the kinesics of inhibition of APN by luteolin was analyzed based on the apparent Michaelis constant ($K_m$app) and maximum reaction rate (V_{max}) of enzymatic reactions, and the inhibition constant K_i was obtained.

Test on inhibition of growth of the HepG2 cells by luteolin

The fumaric reductase in chondriosomes of living cells can reduce the 3-(4,5-dimethyl-thiazol-2)-2,5-diphenyl tetrazolium (MTT) into blue-violet water-insoluble formazan, which is deposited in the cells. Generally, the generation of formazan is positively correlated with the number of living cells under the normal circumstances and is also positively correlated with the cell viability. Formazan can be dissolved by dimethyl sulfoxide (DMSO), and its content can be ascertained by determining the absorption at 570 nm. Therefore, the changes in the determined absorption values at 570 nm can be used to directly predict the number of living cells and find out about the inhibitor or its ability to kill the tumor cells [9].

Bestatin was used as the positive control and the solution without luteolin was used as the blank control. Luteolin at different concentrations and the HepG2 cells were incubated in 5% CO_2 at 37°C for 48 hours. Afterwards, 0.5% MTT solution was added. After 4 h of continuous incubation, centrifugation was performed at 2500 rpm for 30 min. Then the culture medium was discarded, the DMSO solution was added, the UV-2450 UV-visible spectrophotometer was used to detect the absorbance value (OD value) at 570 nm, and the inhibition rate of cell growth was calculated according to the following formula: Inhibition rate (%) = (OD value of the blank-OD value of the inhibitor) × 100%

Determination of fluorescence spectrum

Luteolin solution (0-3.54 × 10^{-4} mol L^{-1}) was continuously added to 3.0 mL of APN solution (2.0 × 10^{-6} mol L^{-1}). At the three temperatures 298, 304 and 310 K, a F-7000 fluorophotometer (Japan Hitachi) was utilized to scan the fluo-

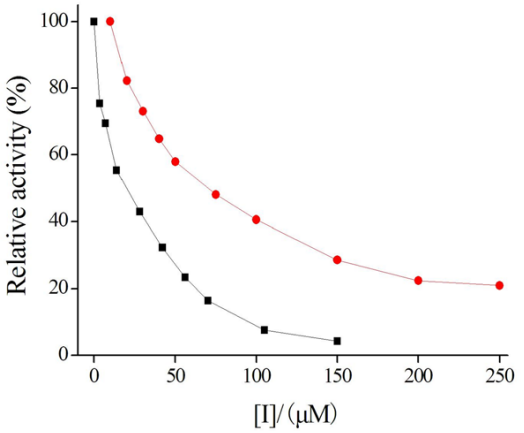

Figure 2. Inhibition of APN by luteolin. (■) = Bestatin, (●) = luteolin, *c*(APN) = 4 μg/mL, *c*(L-leucine aminopeptidase-P-nitroaniline) = 1 × 10^{-3} mol/L.

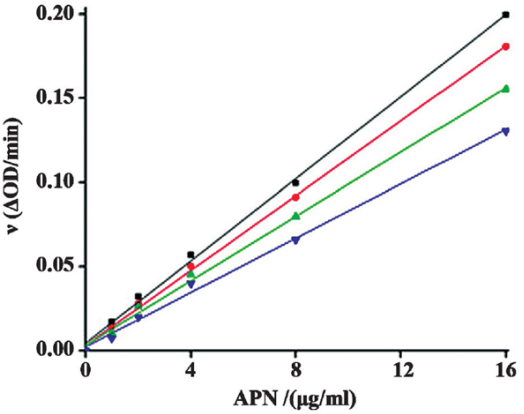

Figure 3. Type of inhibition of APN by luteolin. *c*(L- leucine aminopeptidase-P-nitroaniline) = 1 × 10^{-3} mol/L, *c*(APN) = 4 μg/mL. *c*(luteolin) curve from top down: 0, 25, 75 and 150 μM.

rescence spectrum within the range of 300 to 500 nm with 280 nm as the excitation wavelength, and both of the excitation and emission slits were 2.5 nm.

Determination of circular dichroism

Luteolin at different concentrations was added to the APN solution and mixed well, then the circular dichroism of the sample solution was determined at 37°C, using the phosphate (50 mmol/L) buffer solution (pH 6.8) as blank.

Molecular docking

The molecular modeling simulation software AUTODOCK 4.0 was used for molecular docking between galangin and polyphenol oxidase; APN (PDB:4FKE) was obtained from RCSB Protein Data Bank (http://www.rcsb.org/pdb), and the three-dimensional molecular crystals of luteolin were drawn with the Sybyl × 1.1 software (Tripos Inc., St. Louis, USA). Before molecular docking, the structure and energy of the ligand luteolin and the receptor APN were optimized (dehydrated, hydrogenized and powered), the autogrid box parameter 80 Å × 80 Å × 80 Å was set, and the grid spacing was set as 0.75 Å; Lamarckian genetic algorithm (LGA) was selected for autodock calculation, with default setting for other parameters. The docking was performed for 100 times, and analysis on the results was made using the PyMoL software.

Results and discussion

Inhibition of APN activity by luteolin

As shown in **Figure 2**, the activity of APN decreased continuously as concentration of the inhibitor luteolin increased, and it did not level off until the concentration of luteolin increased to 150 μM, indicating a concentration-dependent inhibition of APN by luteolin; its half maximal inhibitory concentration (IC_{50}) was 70.85 μM, while IC_{50} of the positive control bestatin was 21.23 μM, suggesting that luteolin exhibited some inhibitory effects on APN, consistent with that previously reported in literatures.

Figure 3 showed the relationship between APN activity and amount of the enzyme added. In assay systems with luteolin at different concentrations, a plot was drawn using enzyme activity vs. amount of the enzyme added and a set of straight lines were obtained passing the origin, as the concentration of luteolin increased, the slope of each line continued to decrease, which suggested that increase in concentration of luteolin inhibited the activity of APN, instead of causing decrease in enzyme activity by reducing the effective amount of the enzyme, indicating that the inhibitory effect of luteolin on APN was reversible [10].

Determination on the time course of inhibition of APN by luteolin

In the same buffer system, incubation solution of the same volume was taken for luteolin-enzyme at different concentrations every other 180 s, and the substrate L-leucine aminopepti-

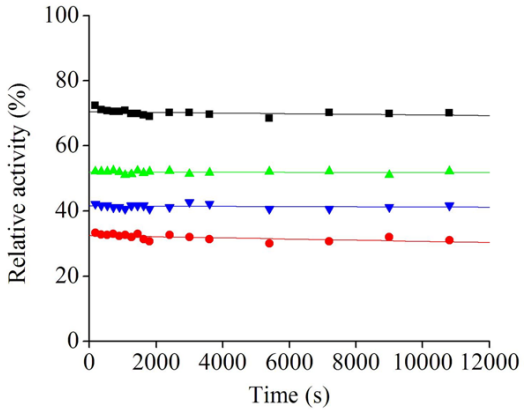

Figure 4. Time course of inhibition of APN by luteolin. *c*(APN) = 4 μg/mL, *c*(luteolin) curve from top down: 0, 75, 100 and 150 μM.

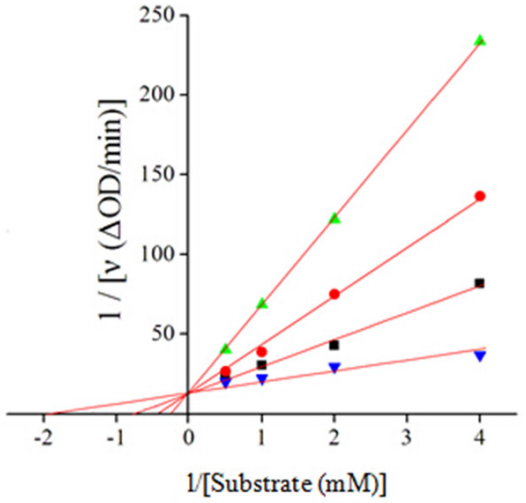

Figure 5. Lineweaver-Burk plot for inhibition of APN by luteolin. *c*(APN) = 4 μg/mL, *c*(luteolin) curve from top down: 0, 75, 100 and 150 μM.

dase-P-nitroaniline was added to determine the time course of APN deactivation. As can be seen from **Figure 4**, at different concentrations of luteolin, there were no changes in the relative activity of APN as the time of incubation prolonged, suggesting that luteolin was ready to interact with APN, changing rapidly the physiological structure and nature of the latter, so that the enzyme was inhibited in a short time and its relative activity did not change with the time of incubation [11].

Kinetic study on inhibition of APN by luteolin

Type of the inhibitory effect of luteolin on APN was further verified. Under the same experimental conditions, the inhibitory effect of luteolin on polyphenol oxidase was investigated at different substrate concentrations to analyze the inhibition kinetics of luteolin on APN, and a plot was drawn with the Lineweaver-Burk double reciprocal equation to obtain the kinetic parameters $K_m$app and V_{max}. As seen in **Figure 5**, the Lineweaver-Burk double reciprocal plot was a set of straight lines intersecting at the ordinate, suggesting that in the system, V_{max} remained unchanged and $K_m$app increased gradually, thus making a kind of typical competitive inhibition [12]. This indicated that luteolin might bind into the active center of APN and compete with substrates for the active sites, thus resulting in an inhibitory effect. On this basis, intercept of the Y-axis was plotted against different concentrations of morin to obtain the inhibition constant K_i = 24.83 μM.

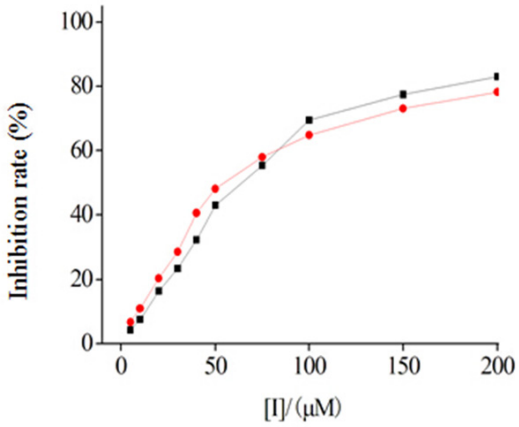

Figure 6. Inhibitory effect of luteolin on growth of the HepG2 cells.

Inhibition of growth of the HepG2 cells by luteolin

APN was the major target of bestatin, which induced apoptosis of the HepG2 cells in acute myeloid diseases. The present study investigated inhibition of the HepG2 cells by luteolin with those cells as the target. Results of the experiment (**Figure 6**) showed that the inhibitory activity of luteolin on the HepG2 cells was consistent with the trend in the experiment on *in vitro* enzyme inhibition, i.e. as the concentration of luteolin increased, the inhibitory effect on the HepG2 cells was markedly enhanced. The half maximal inhibitory concentration (IC_{50}) was 61.23 μM and 49.34 μM respectively for the positive control bestatin and luteolin, and data indicated a slightly higher ability to inhibit

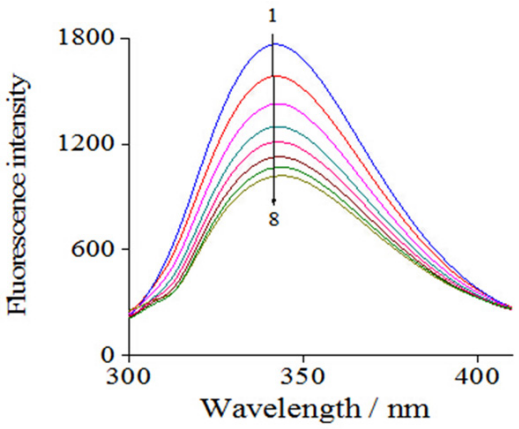

Figure 7. Effects of luteolin on fluorescence emission spectrum of APN. *c*(APN) = 4 μg/mL, *c*(luteolin)/(μM), 1-8: 0, 25, 50, 75, 100, 125, 150 and 175.

Table 1. Effect of luteolin on the secondary structure of APN

[Luteolin] (μM)	α-helix (%)	β-fold (%)	β-turn (%)	Random coil (%)
0	21.2	27.2	21.2	30.4
50	24.8	25.0	21.8	28.4
100	28.2	22.2	22.7	26.9
150	32.9	20.2	22.9	24.0

growth of the HepG2 cells by luteolin than by bestatin, suggesting that luteolin might induce apoptosis of the cells by inhibiting the APN activity.

Effect of luteolin on fluorescence spectrum of APN

By measurement of the changes in fluorescence spectrum of APN in the presence of luteolin, it was found out that as the concentration of luteolin increased, a quenching effect on the endogenous fluorescence of APN was observed in a concentration-dependent manner (**Figure 7**), suggesting possible interaction between the two [13]. The binding parameter of luteolin and APN was obtained and the binding constant at 298 K was calculated as K_a = 3.98 × 10^4 L moL^{-1} using the formula: $\frac{F_0}{F_0 - F} = \frac{1}{f_a K_a}\frac{1}{[Q]} + \frac{1}{f_a}$ [14].

The main forces involved in the interaction of small molecules with biological macromolecules were hydrogen bonding, hydrophobic interaction, van der Waals forces and electrostatic attraction [15]. The type of the main force between small molecules and proteins could be determined from the values of the thermodynamic parameters enthalpy (Δ*H*) and entropy (Δ*S*) changes:

$$\lg K_a = -\frac{\triangle H}{2.303RT} + \frac{\triangle S}{2.303R}$$

In case of no great variability in temperature, enthalpy changes during the reaction could be used as a fixed value to calculate the corresponding Δ*H* and Δ*S* with the van't Hoff equation: ΔG =ΔH-TΔS

Where, K_b was the apparent binding constant at the corresponding temperature and *R* was the gas constant.

1/*T* was plotted against lgK_a, and enthalpy and entropy changes in the system were calculated from the fitted slope and intercept of the straight lines respectively. Free energy changes Δ*G* could be calculated

A thermodynamic analysis was made on the interaction between luteolin and APN and a conclusion was drawn that the binding reaction of the two was a spontaneous process. Δ*H* and Δ*S* were calculated as 36.58 kJ mol^{-1} and 168.12 J mol^{-1} K^{-1} respectively, indicating that the process of luteolin and APN forming complexes was an entropy-driven endothermic reaction and the hydrophobic interaction effort was the main driving force.

Effect of luteolin on the secondary structure of APN

The on-line Dichroweb software was used to calculate the secondary structure content before and after APN binding to luteolin and the results were listed in **Table 1**. As shown in the table, the content of α-helix of free APN was 21.2%, and the content of β-fold was 27.2%. When the concentration of luteolin added to APN was up to 150 μM, the content of α-helix increased to 32.9%, while the content of β-fold decreased to 20.2%, indicating that luteolin induced some changes in the APN conformation. With continuing increase in the content of α-helix, the structure of APN became dense and did not facilitate the process of enzyme forming the active center, resulting in a drop in the activity of APN [16]. This is probably one of

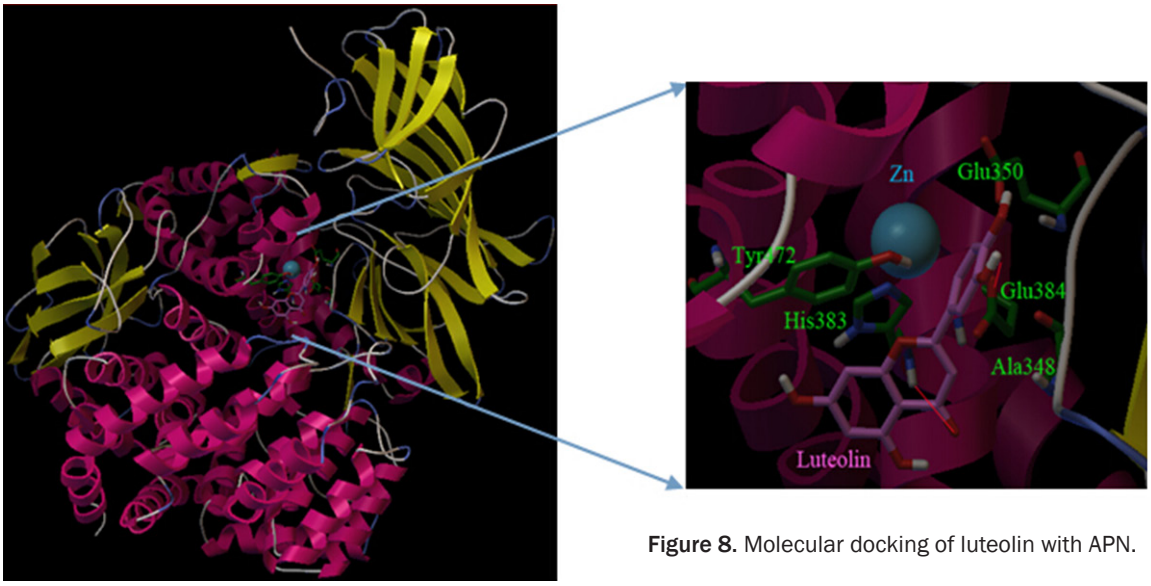

Figure 8. Molecular docking of luteolin with APN.

the mechanisms underlying the inhibition on APN activity by luteolin.

Molecular docking of luteolin with APN

In the results of 100 runs, sites with the most docking regions and the lowest energy were selected for the study and they were also the optimal regions for luteolin binding to APN. As shown in **Figure 8**, luteolin was binding near the active center of zinc ions of APN, fitted into the surrounding areas of the amino acid residues (Ala348, Glu350, His383, Glu384 and Tyr462) in the catalytic center [17], and interacted with His383 and Glu384 to form hydrogen bonds. This implied that luteolin could compete with substrates for the active regions of APN and change the structure of the enzyme, interact with residues in the active center to form hydrogen bonds and subsequently lead to decrease in the catalytic efficiency of APN, which was consistent with the results of the above experiment and was also the mechanism underlying the inhibitory effect of APN on polyphenol oxidase.

Conclusion

It was revealed in the study that luteolin was a reversible competitive inhibitor of APN, with a half maximal inhibitory concentration (IC_{50}) of 70.85 μM and inhibition constant K_i of 21.23 μM; analysis on the time course of inactivation kinetics showed that luteolin could react with APN rapidly to reduce the activity of the enzyme; luteolin had a greater ability to inhibit growth of the HepG2 cells than the positive control bestatin, indicating that luteolin might induce apoptosis of the cells by inhibiting the APN activity; analysis on fluorescence spectrum indicated that the fluorescence of APN was quenched effectively by luteolin, with a binding constant K_a of 3.98×10^4 L mol^{-1} between the two and the hydrophobic interaction force as the main driving force for the interaction; analysis of CD spectra revealed that the binding of luteolin to APN could induce conformational unfolding, causing the content of α-helix to increase, hindering formation of the active center and in turn, leading to reduction in APN activity. In addition, the results of molecular docking further confirmed the validity of the above results that luteolin competitively binds with the active sites of APN, and on the other hand, it can influence the secondary structure of APN, which are the two aspects in the mechanism underlying the inhibition of APN by luteolin.

Disclosure of conflict of interest

None.

Address correspondence to: Enwu Long, Department of Pharmacy, Sichuan Academy of Medical Sciences & Sichuan Provincial People's Hospital, Chengdu 610072, China. E-mail: longenwuscph@sina.com

References

[1] Folkman J. Seminars in Medicine of the Beth Israel Hospital, Boston. Clinical applications of research on angiogenesis. N Engl J Med 1995; 333: 1757-1763.

[2] Dong X, An B, Salvucci KL, Storkus WJ, Amoscato AA and Salter RD. Modification of the amino terminus of a class II epitope confers resistance to degradation by CD13 on dendritic cells and enhances presentation to T cells. J Immunol 2000; 164: 129-135.

[3] Larsen SL, Pedersen LO, Buus S and Stryhn A. T cell responses affected by aminopeptidase N (CD13)-mediated trimming of major histocompatibility complex class II-bound peptides. J Exp Med 1996; 184: 183-189.

[4] Pasqualini R, Koivunen E, Kain R, Lahdenranta J, Sakamoto M, Stryhn A, Ashmun RA, Shapiro LH, Arap W and Ruoslahti E. Aminopeptidase N is a receptor for tumor-homing peptides and a target for inhibiting angiogenesis. Cancer Res 2000; 60: 722-727.

[5] Saiki I, Yoneda J, Azuma I, Fujii H, Abe F, Nakajima M and Tsuruo T. Role of aminopeptidase N (CD13) in tumor-cell invasion and extracellular matrix degradation. Int J Cancer 1993; 54: 137-143.

[6] Wang Y, Zhang G, Yan J and Gong D. Inhibitory effect of morin on tyrosinase: Insights from spectroscopic and molecular docking studies. Food Chem 2014; 163: 226-233.

[7] Kimata M, Shichijo M, Miura T, Serizawa I, Inagaki N, Nagai H. Effects of luteolin, quercetin and baicalein on immunoglobulin E-mediated mediator release from human cultured mast cells. Clin Exp Allergy 2000; 30: 501-508.

[8] Ko WG, Kang TH, Lee SJ, Kim YC and Lee BH. Effects of luteolin on the inhibition of proliferation and induction of apoptosis in human myeloid leukaemia cells. Phytother Res 2002; 16: 295-298.

[9] Liu Y, Shang L, Fang H, Zhu H, Mu J, Wang Q, Wang X, Yuan Y and Xu W. Design, synthesis, and preliminary studies of the activity of novel derivatives of N-cinnamoyl-l-aspartic acid as inhibitors of aminopeptidase N/CD13. Bioorg Med Chem 2009; 17: 7398-7404.

[10] Jeong SH, Ryu YB, Curtis-Long MJ, Ryu HW, Baek YS, Kang JE, Lee WS, Park KH. Tyrosinase Inhibitory Polyphenols from Roots of Morus lhou. J Agric Food Chem 2009; 57: 1195-1203.

[11] Lü ZR, Long S, Wang J, Park D, Bhak J, Yang JM, Park YD, Zhou HW and Fei Z. The effect of trifluoroethanol on tyrosinase activity and conformation: inhibition kinetics and computational simulations. Appl Biochem Biotechnol 2009; 160: 1896-1908.

[12] Qiu L, Chen QH, Zhuang JX, Zhong X, Zhou JJ, Guo YJ and Chen QX. Inhibitory effects of α-cyano-4-hydroxycinnamic acid on the activity of mushroom tyrosinase. Food Chem 2009; 112: 609–613.

[13] Yan J, Zhang G, Hu Y and Ma Y. Effect of luteolin on xanthine oxidase: Inhibition kinetics and interaction mechanism merging with docking simulation. Food Chem 2013; 141: 3766-3773.

[14] Skrt M, Benedik E, Podlipnik Č and Ulrih NP. Interactions of different polyphenols with bovine serum albumin using fluorescence quenching and molecular docking. Food Chem 2012; 135: 2418-2424.

[15] Ross PD and Subramanian S. Thermodynamics of protein association reactions: forces contributing to stability. Biochem 1981; 20: 3096-3102.

[16] Yoshimori A, Oyama T, Takahashi S, Abe H, Kamiya T, Abe T and Tanuma SI. Structure-activity relationships of the thujaplicins for inhibition of human tyrosinase. Bioorg Med Chem 2014; 22: 6193-6200.

[17] Chen L, Lin YL, Peng G and Li F. Structural basis for multifunctional roles of mammalian aminopeptidase N. Proc Natl Acad Sci U S A 2012; 109: 17966-17971.